



Dynamic optimization of personal exposure and energy consumption while ensuring thermal comfort in a test house

Nishchaya Kumar Mishra ^a, Marina E. Vance ^b, Atila Novoselac ^c, Sameer Patel ^{a,d,e,*}

^a Department of Civil Engineering, Indian Institute of Technology Gandhinagar, Palaj, Gandhinagar, Gujarat, 382355, India

^b Department of Mechanical Engineering, University of Colorado Boulder, Boulder, CO, 80309, United States

^c Department of Civil, Architectural, and Environmental Engineering, University of Texas at Austin, Austin, TX, 78712, United States

^d Department of Chemical Engineering, Indian Institute of Technology Gandhinagar, Palaj, Gandhinagar, Gujarat, 382355, India

^e Kiran C. Patel Centre of Sustainable Development, Indian Institute of Technology Gandhinagar, Palaj, Gandhinagar, Gujarat, 382355, India



ARTICLE INFO

Keywords:

Dynamic optimization
Energy-exposure trade-off
Indoor air pollution mitigation
Thermal comfort
Personal exposure

ABSTRACT

Owing to significant time spent indoors, indoor air quality (IAQ) and thermal comfort are critical to ensure occupants' well-being. Buildings already account for a considerable fraction of developed nations' energy consumption, primarily for maintaining thermal comfort. Measures to improve IAQ can further increase the energy demand. Thus, optimizing IAQ, energy consumption, and thermal comfort is critical. This work presents a dynamic optimization model to investigate the complex and interdependent relationship between personal exposure to particulate matter (PM), thermal comfort, and energy consumption in a test house during typical cooking activities and intense holiday cooking. Surface deposition dominated PM removal for both scenarios (72–78 %). During optimization of the cost function with higher weightage for exposure, exfiltration became the primary PM removal mechanism due to the increased outdoor-indoor air change rate. However, this also increased air conditioning energy consumption. Adding a filter to the recirculation system and increasing the indoor set temperature can save energy while maintaining the same level of exposure reduction achieved via exfiltration alone. Simulations corresponding to higher outdoor temperatures demonstrated that increasing the indoor set temperature from 25°C to 27°C reduces exposure and energy consumption relative to the benchmark without considerable compromise to the comfort level. A high normalized exposure reduction results in an energy-efficient system but might not always translate to a desirable exposure reduction, thus indicating an energy-exposure trade-off.

1. Introduction

Owing to significant time spent indoors [1–4], a healthy and comfortable indoor environment for occupants' productivity [4,5], health and well-being [6–11], and comfort [12–15] becomes imperative. Allen et al. discuss the case for healthy buildings and the need for integration of health performance indices and have proposed nine foundations, including good indoor air quality (IAQ), acoustic comfort, and thermal comfort [4,5]. Indoor air pollutants (IAPs) like volatile organic compounds (VOCs), particulate matter (PM), and NO_x associated with health implications such as chronic obstructive pulmonary disease (COPD), asthma, acute respiratory infections (ARI) and several other respiratory dysfunctions [16–19], directly impact mortality and morbidity [7]. Kephart et al. [16] demonstrate that 69 % of 24-h samples

exceeded the World Health Organization (WHO) indoor annual NO₂ concentration guidelines, and 47 % of samples exceeded WHO indoor hourly guidelines. As per the WHO, around 3.2 million premature annual deaths are attributable to illnesses from indoor air pollution [20]. IAQ is governed by multiple pollutants such as PM, VOCs, NO_x, and other gaseous pollutants, all with varying contributions to illnesses and mortality. PM is the most widely studied air pollutant due to its dynamic physicochemical characteristics, role in environmental processes, and severe health implications. PM varies considerably in size, which governs its transport characteristics and health impacts. Coarse PM has an aerodynamic diameter greater than 2.5 μm, and sub-2.5 μm PM (PM_{2.5}) is classified as fine PM. A subset of PM_{2.5}, sub-100 nm particles are referred to as ultrafine PM. Fine PM (PM_{2.5}) is of health concern as it can penetrate deeper into our lungs, posing more risk to our health than coarse PM [10,21,22]. Within PM_{2.5}, smaller PM providing a

* Corresponding author: Department of Civil Engineering, Indian Institute of Technology Gandhinagar, Palaj, Gandhinagar, Gujarat, 382355, India.

E-mail address: sameer.patel@iitgn.ac.in (S. Patel).

Abbreviations	
AHU	Air Handling Unit
ARI	Acute Respiratory Infection
ASHRAE	American Society for Heating, Refrigeration and Air Conditioning Engineers
BM	Benchmark
COPD	Chronic Obstructive Pulmonary Disease
DASS	Dedicated Air Supply System
EER	Energy Efficiency Ratio
ER	Emission Rate
HOMEChem	House Observations of Microbial and Environmental Chemistry
HVAC	Heating, Ventilation and Air Conditioning
IAP	Indoor Air Pollutant
IAQ	Indoor Air Quality
IR	Infiltration Rate
LD	Layered Day
NER	Normalized Exposure Reduction
NO _x	Nitrogen Oxides
NREL:	National Renewable Energy Laboratory
PM	Particulate Matter
RH	Relative Humidity
SMPS	Scanning Mobility Particle Sizer
TGD	Thanksgiving Day
VOC	Volatile Organic Compound
WHO	World Health Organization

higher specific surface area might be more harmful as recent studies have reported the surface area of PM to be better associated with health impacts [10,23–25]. Sub-500 nm PM usually dominates the total PM levels in indoor environments [9,11,26,27].

Apart from good IAQ, desirable thermal comfort should be ensured for the well-being of the occupants. Initial building designs focused on passive ventilation for air circulation and thermal comfort [13,28]. The concept of thermal comfort in the indoor environment has evolved from directly controlling the microclimate of the indoor environment to adaptive comfort based on learning and validating the adaptive setting points and standards [13]. The advent of HVAC (heating, ventilation, and air conditioning) systems provided finer control over thermal comfort. Buildings with HVAC systems are relatively air-tight, and air change rates are strictly controlled to maintain desirable thermal comfort conditions [28,29]. However, the air-tight envelope of buildings, which reduces the infiltration of outdoor pollutants, also restricts IAPs from escaping the indoor environment. Furthermore, the reduced dilution of indoor air leads to elevated indoor concentrations of pollutants of indoor origin. Therefore, buildings should have sufficient outdoor-indoor air change rates to maintain a fresh air supply. Guidelines for minimum ventilation rates are stipulated by ASHRAE (American Society for Heating, Refrigeration and Air Conditioning Engineers) [30]. However, ASHRAE-recommended air change rates might be insufficient to minimize exposure in indoor environments [4,5,31,32]. Therefore, an increased outdoor-indoor air change rate is required to transport indoor pollutants outdoors. This increased air change rate is based on the premise that the outdoor environment is cleaner than indoors. However, recent studies have shown that pollutants of outdoor origin dominate or contribute equally to exposure in indoor spaces [3, 33–38]. Wallace et al. [37] and Lunderberg et al. [38] demonstrated that indoor sources account for around 50 % of total indoor PM_{2.5}, thus presenting the need for a controlled air change between indoor and outdoor environments.

HVAC operation is energy intensive, accounting for more than 50 % of total building energy consumption, as demonstrated by multiple studies [39–44]. The increased outdoor-indoor air change for reducing indoor pollutant concentrations further increases the HVAC energy consumption due to additional air conditioning or heating required to maintain thermal comfort. Therefore, a trade-off exists between personal exposure, energy consumption, and thermal comfort, making it critical to understand the trade-off and its optimization by investigating their interdependency.

Recent studies have proposed specific control strategies such as dynamic optimization, moving horizon estimate, and predictive control for achieving optimal operating conditions to meet the stipulated concentration levels and thermal comfort with minimum energy consumption in a range of built environments, including residential [45–49], subway systems [50], education institutes [12], and healthcare centers [15]. For

example, Ganesh et al. employed a dynamic optimization strategy to control indoor pollutants and reported a peak PM concentration reduction of 31 % and AHU energy consumption of 17.7 % [46]. However, thermal comfort was not accounted for in the same study; thus, the reduced consumption might come at the cost of occupants' comfort. Hou et al. deployed a hybrid prediction model to predict and optimize IAQ, thermal comfort, and energy consumption; however, CO₂ was the sole parameter for measuring IAQ [14]. Another study by Xu et al. examined the feasibility of predictive control techniques for indoor environment quality based on thermal comfort adaption using CO₂ as the only IAQ metric [51]. Considering only CO₂ as a proxy for IAQ might not be suitable since other ubiquitous indoor pollutants have more serious health impacts. Optimization and control strategies primarily focusing on critical indoor pollutants such as PM, NO_x, and VOCs conjugated with energy and thermal comfort in residential buildings are limited.

In summary, elevated PM levels (especially sub-micron) in indoor environments pose a significant health risk to occupants. Reliance on outdoor-indoor air change rate to reduce indoor PM levels translates to increased energy consumption to maintain thermal comfort when a temperature difference exists between indoor and outdoor environments, thus presenting a dynamic and complex interdependent system. Therefore, it is critical to devise control strategies for indoor PM while optimizing for associated energy consumption and thermal comfort. This study presents a dynamic optimization-based model to evaluate the trade-off between PM exposure, energy consumption, and thermal comfort in a test house. The measured PM emission rates and other test house parameters from the House Observations of Microbial and Environmental Chemistry (HOMEChem) study have been used as model inputs [9,11,52,53]. Simulations are performed for two experiments representing typical intermittent cooking patterns and intense cooking activities. Parametric and sensitivity analyses are performed for different model constraints to assess their impacts on the energy-exposure relationship. Specifically, the study quantifies (1) the energy intensiveness of exposure reduction, (2) the interdependency of thermal comfort and elevated pollutant concentration to reduce the energy penalty, and (3) the efficacy of filters and subsequent impacts on the energy-exposure relationship.

2. Materials and methods

2.1. Test house, experimental setup, and instrumentation

The HOMEChem study was a field campaign conducted in a manufactured test house in June 2018 to investigate the impacts of everyday activities on indoor air quality and indoor chemistry in a semi-controlled residential environment [52]. More details about the test house characteristics and operating conditions, experimental design, instrumentation, and source characterization are discussed in previous

HOMEChem studies [9,11,52]. Briefly, the test house is located at the University of Texas at Austin and has a floor area of $\sim 111 \text{ m}^2$ and a volume of $\sim 250 \text{ m}^3$. A dedicated air supply system (DASS) maintained an outdoor air change rate of $0.5 \pm 0.1 \text{ h}^{-1}$ when the house had closed doors and windows. The HVAC system of the test house is representative of a typical residential system providing cooling, dehumidification, and air circulation. The air handling unit (AHU) of the HVAC system was operated continuously without a filter to avoid impact of filter selection on experimental results and enable to focus experiments on indoor chemistry. The AHUs flow rate of $2000 \text{ m}^3 \text{ h}^{-1}$, equivalent to 8 h^{-1} , and continuous AHU's fan operation allowed good air mixing and relatively small spatial gradients. Section S1 of the supplementary information (SI) contains key test house parameters and relevant discussion.

The presented model is applied to two types of experiments - Layered Day (LD) and Thanksgiving Day (TGD). LD simulated a real-life day in residential environments, including cooking three meals (breakfast, lunch, and dinner) and floor mopping. TGD included preparing a typical American Thanksgiving meal for about 14 persons. A combination of particle sizers measured particle size distributions ($\sim 1 \text{ nm}$ – $20 \mu\text{m}$) [11]. Particle source strengths, infiltration rates, and deposition rates were used as input for this study. These values were modeled by Patel et al. [9] using size-resolved (4–500 nm) particle concentration measurements from two Scanning Mobility Particle Sizers (SMPS, TSI Inc., Shoreview, MN) collected at a 5-min resolution. For LD, the PM_{0.5}/PM_{2.5} ratio varied between 0.43 and 0.89 over the cooking duration [11]. During Thanksgiving Day, the PM_{0.5}/PM_{2.5} ratio was 0.93 when averaged over 12 h (8 a.m.–8 p.m.) [11] demonstrating that most of the PM of indoor origin was sub-500 nm, justifying the choice of going with PM_{0.5} instead of other cut-off sizes such as PM_{0.1}, PM₁, and PM_{2.5}.

2.2. Indoor PM dynamics

Fig. 1 presents a schematic of the test house with a DASS for outdoor air change and a HVAC system for recirculation and air conditioning. Eq. (1) represents a material balance model for PM concentration in a well-mixed volume [54].

$$\frac{dC}{dt} = \frac{IR}{V} - \lambda_{DASS} C + \frac{ER}{V} - (1-p) C \lambda_{HVC} - \gamma C \quad (1)$$

Where C is indoor PM concentration ($\mu\text{g}/\text{m}^3$), IR is the infiltration rate of outdoor PM ($\mu\text{g}/\text{min}$), λ_{DASS} is indoor-outdoor air change rate (min^{-1}), ER is the emission rate of PM from indoor sources ($\mu\text{g}/\text{min}$), V is the volume of the test house (m^3), p is the PM penetration factor for the HVAC filter, λ_{HVC} is recirculated air change rate (min^{-1}), and γ is PM surface deposition rate (min^{-1}).

Patel et al. [9] reported size and time-resolved ERs corresponding to LD and TGD for sub-500 nm particles. This work uses these ERs to

calculate cumulative mass ERs that serve as input for all simulations. Mass-based ERs reported at 5-min resolution are converted to 1-min resolution assuming constant emissions for five data points. Patel et al. [9] also reported the size-resolved IR of aerosols corresponding to an outdoor-indoor air change rate equivalent to 0.5 h^{-1} . Since IR varies with ambient PM concentration and outdoor-indoor air change, this work assumes a linear relationship between IR and the outdoor-indoor air change rate. More discussion about this is available in Section S2.

Patel et al. [9] also reported the size-resolved deposition rates accounting for particle losses or deposition in the HVAC system. Therefore, p in Eq. (1) can be said to be one, and γ includes the non-zero penetration factor of the HVAC system. Since the present work simulates cumulative PM mass concentration, size-resolved γ from the previous work cannot be directly used. A sensitivity analysis was performed for different γ values simulating PM_{0.5} for 24 h and comparing it with measurements. γ values for which simulated 24-h exposure was close to that measured were chosen for LD (1.80 h^{-1}) and TGD (1.269 h^{-1}). A detailed discussion on the estimation of infiltration rates, deposition rates, and emission rates is presented in Section S2.

2.3. Energy balance model

2.3.1. Operation of HVAC system

An HVAC system, consisting of an AHU and air conditioning unit, regulated the indoor temperature of the test house. The AHU provided a continuous recirculation (equivalent to 8 h^{-1}), and the air conditioning unit operated intermittently to maintain the indoor temperature of 25°C . The outdoor air through the DASS (equivalent 0.5 h^{-1}) was mixed with the return air of the HVAC system before the air conditioning unit (**Fig. 1**). There was no single outlet channel (as depicted in **Fig. 1**). The test house was positively pressurized. The indoor air left the test house envelope via cracks and openings.

The air conditioning unit operated whenever the indoor temperature exceeded the set temperature (25°C). The extent of cooling depends on the capacity of the air conditioning unit and the thermodynamic properties of the mixed air (outdoor air and return air). **Fig. S3** shows the measured temperature and RH of return air and supply air in the test house. Based on **Fig. S3**, the air conditioning system operation is modeled with three constraints: (1) the maximum temperature difference for supply and return air cannot exceed 10°C , (2) the minimum temperature of supply air is 15°C , and (3) the RH of supply air is 90 %. Further, the capacity and power consumption of air conditioning unit depends on factors such as floor area, the system's energy efficiency ratio (EER), and climatic zones [55]. The capacity of the HVAC system and its efficiency ratio for modeling the system are adopted based on the evaluation of the residential HVAC system proposed by Do et al. [55]. **Fig. S4** summarizes the modeled operation strategy of the HVAC system.

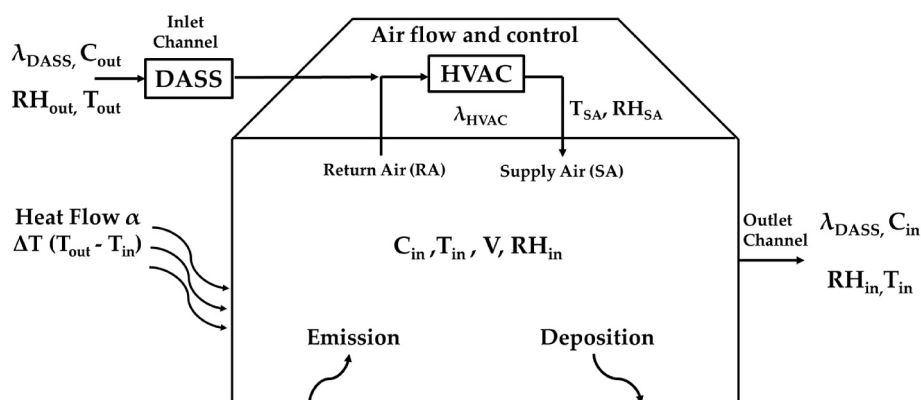


Fig. 1. Schematic of the test house depicting dedicated air supply system (DASS), heating, ventilation and air conditioning (HVAC), and various indoor and outdoor parameters. in: indoor, out: outdoor, λ : air change rate, C : PM concentration, RH: relative humidity, T : air temperature, V : room volume.

2.3.2. Power consumption of HVAC and DASS

An energy balance is applied to estimate indoor air temperature and RH, which are governed by outdoor air properties, operation of the HVAC system, and heat transfer from outdoors. The net enthalpy change for the indoor air is expressed using Eq. (2) [56,57].

$$\frac{dh_{in}}{dt} = (\lambda_{DASS} + \lambda_{HVAC}) (h_{SA} - h_{in}) + \alpha \frac{T_{out} - T_{in}}{V \rho_{air}} \quad (2)$$

h_{in} and h_{SA} are indoor air and supply air enthalpy, respectively; α is a measure of the thermal permeability of the house, and ρ_{air} is air density. The first term represents the enthalpy change due to the supply air, and the second is the heat transfer due to the differences between outdoor and indoor temperatures. The value of α for a house depends on factors such as elements of the house and material used, dimensions of various features such as doors and windows, and geographical location. A passive solar design strategy for residential buildings by the National Renewable Energy Laboratory (NREL), USA, estimates various associated heat losses and thermal permeability of typical houses in the same geographical region as the test house [58]. The discussion of the thermal properties of the house is not the primary focus of this study. Hence, a representative α value of $0.068 \text{ kW}^{\circ}\text{C}$ is adopted based on the test house location, i.e., Austin, Texas [58]. Moreover, this model does not account for internal heat sources such as occupants' body heat and that emitted from appliances. While it is acknowledged that the choice of α value and exclusion of internal heat sources can affect the absolute values of simulation results, this work focuses on comparative analyses with the benchmark conditions. The benchmark data used here does not include internal heat sources and has been obtained using the same α value. Therefore, excluding the indoor heat sources and approximating the α value should not affect the insights and results presented here. The outdoor air temperature and RH were measured during HOMEChem experiments, and the same is used for simulations in this study.

Further, Eq. (3) is applied to estimate the changes in the water content of the indoor air due to mixing with outdoor air and air conditioning [59,60].

$$\frac{dw_{in}}{dt} = (\lambda_{DASS} + \lambda_{HVAC}) (w_{SA} - w_{in}) \quad (3)$$

Where w_{in} and w_{SA} are the water content of indoor air and the supply air, respectively. The indoor air temperature is derived from the empirical relationship between various thermodynamic properties of air (Eq. (4)) [56]. More details about Eq. (4) and the estimation of RH are discussed in Section S3.

$$T = \frac{h - 2.5 \omega}{1.01 + 0.00189 \omega} \quad (4)$$

where T is the temperature and ω is the specific humidity of indoor air.

Power consumption of DASS (outdoor-indoor air flow) and HVAC (recirculation and air conditioning) are calculated for each simulation. The energy consumption of the air conditioning unit is a function of enthalpy change between mixed air and supply air. The enthalpy of mixed air entering the HVAC system is given by Eq. (5), and the enthalpy of supply air is similarly estimated using Eq. (6) [56].

$$h_{mixed} = \frac{\lambda_{DASS} h_{out} + \lambda_{HVAC} h_{in}}{\lambda_{DASS} + \lambda_{HVAC}} \quad (5)$$

$$h_{SA} = T_{SA} (1.01 + 0.00189 \omega_{SA}) + 2.5 \omega_{SA} \quad (6)$$

The power consumption of the DASS and the AHU unit for recirculation is a function of flow rates, pressure drops, and efficiencies. Total energy consumption (E) is thus estimated using Eq. (7).

$$E = \frac{\rho_{air} \lambda_{HVAC} V (h_{mixed} - h_{SA})}{EER} + \frac{\Delta P_{HVAC} \lambda_{HVAC} V}{\eta_{HVAC}} + \frac{\Delta P_{DASS} \lambda_{DASS} V}{\eta_{DASS}} \quad (7)$$

Where ΔP_{HVAC} and ΔP_{DASS} are pressure drops across the AHU and DASS,

respectively, and η_{HVAC} and η_{DASS} are the AHU and DASS efficiencies. The pressure drops and efficiency values are adopted from Patel et al. [9].

2.4. Benchmark and optimization of cost function

The physics-based model formulated in the above sub-sections is used to construct temporal indoor PM profiles and model the operation of DASS and HVAC systems similar to experimental conditions for both LD and TGD. Even though the PM concentration was measured, the same is also simulated using previously reported emission rates and household characteristics [9,52]. The simulated concentration profile and resultant exposure agree well with the measurements demonstrated in Section S4. The same simulations also estimated the energy consumption of DASS and HVAC operation for both days under experimental conditions. The simulated PM profile, cumulative exposure, and energy consumption are used as a benchmark for all the simulations carried out in this work. Simulated benchmark data and its comparison with measurements are discussed in Section S4.

The cost function (Eq. (8)) has two components. The first component is energy consumption, and the second is a measure of PM concentration and, therefore, personal exposure. C_{max} is the defined threshold for indoor PM concentration. The optimization strategy aims to operate the DASS and HVAC to optimize the trade-off between reduction in exposure and increased energy consumption to maintain thermal comfort. The cost function can be expressed mathematically as

minimize

$$obj = W_1 E + W_2 (\max(0, C - C_{max}))^a \quad (8)$$

subjected to $\lambda_{min} \leq \lambda_{DASS} \leq \lambda_{max}$

Model Eq. 1 to 7

where λ_{min} (0.5 h^{-1}) and λ_{max} (10 h^{-1}) are the lower and upper bounds of the outdoor-indoor air change rate, respectively. The lower bound of λ_{DASS} is per ASHRAE's requirements [61], and the upper bound is kept at 10 h^{-1} for the simulations while acknowledging that obtaining such high air change rates might not be feasible from the typical residential scale DASS. W_1 and W_2 are user-defined weightage factors for the energy and exposure components of the optimization function. The assigned weightage (W_1 , W_2) determines the goal of optimization, i.e., the component assigned higher weight is minimized preferably. Distinct W_1/W_2 ratios will result in contrasting operating conditions of DASS and HVAC, which govern personal exposure and energy consumption. The following section discusses the sensitivity analysis of personal exposure and energy consumption to W_1/W_2 .

3. Results and discussion

3.1. Sensitivity analysis of weights (W_1 and W_2) in cost function

Multi-objective optimization problems like Eq. (8) do not necessarily give an optimal solution that simultaneously minimizes all the objectives. Owing to conflicting objectives, the optimal parameters of some objectives may not lead to the optimality of the other objectives. These conflicts lead to trade-offs and need a certain balance of the objectives [62,63]. The comparison of objectives and estimation of trade-offs (interdependency) require reformulation, and often, a scalar-valued function with a weighted combination of all objectives is used [46,47,62–64]. The weighted sum method combines all cost functions in one composite cost function using different weightage to different objectives. Ganesh et al. [46,47] used weightage of 1 and 10 for energy and exceedance of pollutant concentration, respectively, while formulating an optimization strategy to control indoor air pollutant levels. The optimal solution strongly depends on the assigned weighting

combination. Various studies have empirically chosen different weighting combinations, and there is no generally applicable method for choosing these combinations [46,47,50,64].

Unlike energy consumption, quantifying the health impacts of exposure to indoor PM is complex. Therefore, choosing weightage factors, i.e., W_1 and W_2 , is not straightforward. This section presents energy and exposure sensitivity analyses by varying W_1/W_2 ratios from 0.01 to 100. For all simulations discussed here, the widely accepted a -value of 2 and a value of $10 \mu\text{g}/\text{m}^3$ for allowable or target indoor PM concentration (C_{\max}) is used in Eq. (8). Section S5 discusses the choice of a -value and C_{\max} along with sensitivity analyses.

The sensitivity analysis in Fig. 2 demonstrates higher exposure reductions for lower W_1/W_2 ratios. For example, $W_1/W_2 = 0.01$, i.e., 100 times more weightage to exposure reduction than energy savings, resulted in 37 % and 75 % exposure reduction compared to the benchmark case for LD and TGD, respectively. However, the exposure reduction comes with an energy penalty due to the increased cooling demand induced by the DASS operation to maintain higher indoor-outdoor air change rates. For the same case ($W_1/W_2 = 0.01$), energy consumption increased by 13 % and 100 % for LD and TGD, respectively. In contrast, $W_1/W_2 = 100$, representing 100 times more weightage to energy savings, resulted in an exposure reduction of 27 % and 70 % for LD and TGD, respectively. Correspondingly, energy consumption increased by 4.5 % and 63 % for respective cases. Even with considerable differences in the weightage ($W_1/W_2 = 100$ vs. $W_1/W_2 = 0.01$), reductions in exposure for TGD are comparable (70 % and 75 %) but with considerable differences in energy penalty (63 % and 100 %). Such trends demonstrate diminishing marginal returns in terms of exposure reduction for every unit of additional energy consumption.

To further discuss diminishing marginal returns, normalized exposure reduction (NER; Fig. 2B and D), i.e., the percentage exposure reduction normalized by the percentage increase in energy consumption, is calculated. For both LD and TGD, NER increases monotonically with W_1/W_2 ratio. Higher values of NER (for high W_1/W_2 ratios)

indicate greater efficiencies, i.e., a larger extent of exposure reduction for the same energy penalty. However, high NERs might not translate to desirable exposure reductions in absolute terms, as demonstrated in Fig. 2A and C. High NERs for high W_1/W_2 ratios are due to the first-order decay nature of PM via deposition and exfiltration. PM levels are high when $W_1 \gg W_2$, which translates to a higher reduction in PM levels in the same duration if other factors are kept constant.

The energy-exposure relationships discussed in this section are based on the premise that the thermal comfort of occupants is not compromised, which means that the HVAC system operates to maintain the set indoor temperature (25 °C during experiments). Hence, the additional energy consumption can be primarily attributed to the HVAC operation governed by the set temperature. An additional increase in energy consumption due to personal exposure reduction will further add to the ever-increasing cooling demand globally. Therefore, the following section discusses the impacts of thermal comfort standards on the energy-exposure nexus.

3.2. Sensitivity of energy and exposure to set temperature

A significant fraction of total energy consumption is associated with the HVAC operation to maintain a set indoor temperature (discussed in the previous section and Section S4). Based on the sensitivity analysis of the energy-exposure nexus, additional energy consumption to reduce personal exposure is inevitable when air conditioning is required. Thus, reducing exposure with minimum energy cost requires a reduced cooling demand. One way to achieve this is to have higher indoor set temperatures, which govern the thermal comfort of occupants. The occupants' awareness and satisfaction with the thermal environment govern the perceived thermal comfort. Recent studies have discussed the concept of adaptive thermal comfort and identified a range of indoor temperature and RH combinations that meet thermal comfort conditions with varying levels of satisfaction [13,65–69]. Another study on adaptive thermal comfort by Karyono et al. [13] summarizes multiple

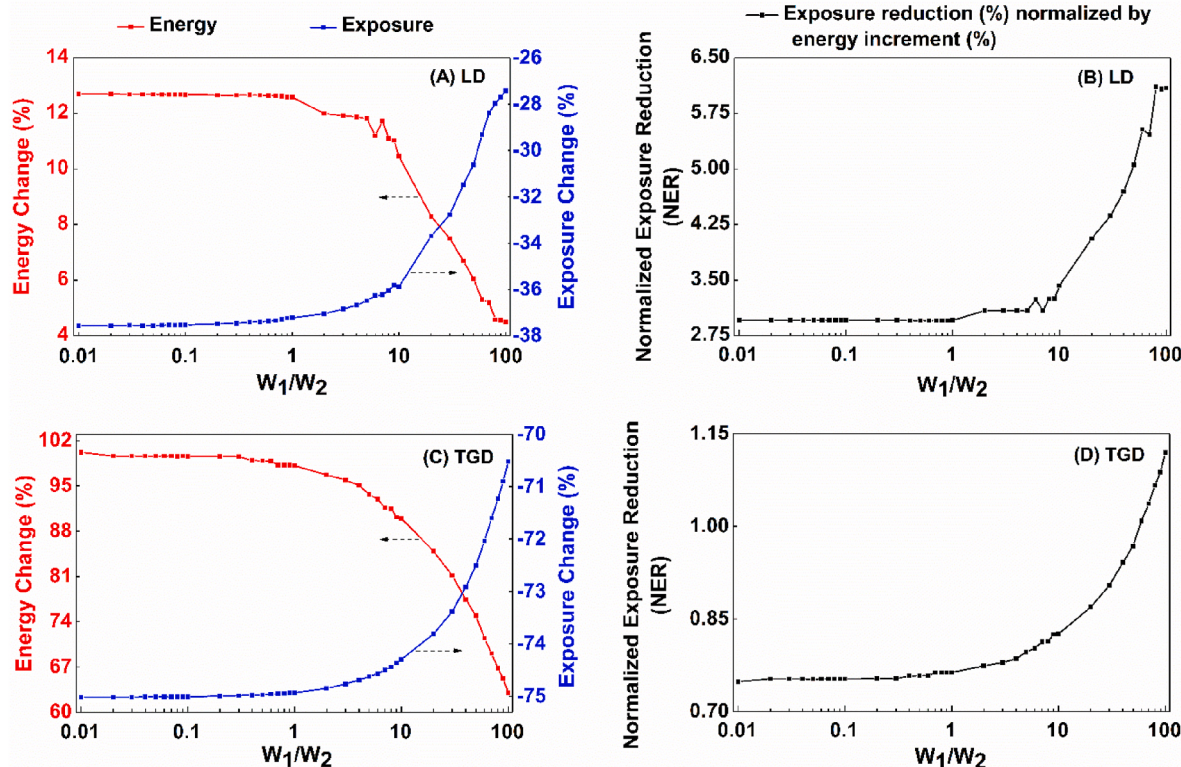


Fig. 2. Sensitivity analysis of energy and exposure for LD and TGD with distinct W_1/W_2 ratios where (A) and (C) are energy-exposure sensitivity, and (B) and (D) are variations of normalized exposure reduction (NER). (+)ve change means increment, and (-)ve change means reduction.

comfort zones on the psychrometrics chart based on the predicted mean vote – percentage person dissatisfied (PMV-PPD) model adopted in ASHRAE-55 [65] and Giovni comfort zones [70]. The PMV-PPD model is widely used to describe the thermal comfort conditions for human occupants. The PPV and PPD indices depend on factors such as air velocity, air temperature, air relative humidity, mean radiant temperature, activity level, and clothing level [65]. The ASHRAE comfort conditions specify different comfort zones for different combinations of temperature ranging from 21 °C to 28 °C and RH ranging from 80 % to 50 %. Therefore, a reasonably wide range of temperatures and RH can ensure occupants' comfort. Here, a simplified model of discomfort index dependent on temperature and humidity is adopted, which is discussed in Section S6.

During HOMEChem experiments, the set temperature was 25 °C. Simulations are performed to assess energy penalty sensitivity to varying set temperatures (23–28 °C) for four optimization cases ($W_1/W_2 = 1/50$, 1/3, 3, and 50). The results are summarized in Fig. 3. The energy consumption trends are intuitive since the lower set temperatures demonstrate higher energy consumption and vice-versa. Section S6 and Fig. S9 discuss the impacts of increased set temperature on occupants' comfort using a discomfort index metric that accounts for both the temperature and RH. Even for the worst-case scenario, i.e., $T_{set} = 28^\circ\text{C}$ and $W_1/W_2 = 1/50$ (high outdoor-indoor air change), the discomfort index remained within the desirable limits for LD and TGD (Fig. S9 C and F).

The set temperature governs the frequency and duration of HVAC operation, affecting energy consumption and, thus, the trade-off between energy and exposure in the optimization problem. Table S4 demonstrates that variations in exposure reduction are minor even if the set temperature is varied from 23 °C to 28 °C for the same W_1/W_2 ratios. This trend indicates the limited dependency of exposure reduction on the set temperature while applying dynamic optimization (Eq. (8)). In contrast, the energy consumption patterns vary linearly with the set temperature corresponding to any W_1/W_2 ratio (Fig. 3 and Fig S10). The highest energy consumption increase (38 % for LD and 166 % for TGD) is observed for the lowest set temperature compared to the benchmark. On the other hand, 20 % of energy can be saved if the set temperature is 28 °C for LD. However, for TGD, the energy consumptions are significantly higher relative to benchmark even when the set temperature is 28 °C owing to the elevated indoor PM concentration that governs the dynamics of the optimization problem (Eq. (8)). Now consider a W_1/W_2 ratio of 3 where the exposure reduction of ~37 % and ~75 % is achieved for LD and TGD, and maintaining the benchmark set temperature (25 °C) requires additional energy consumption of 12 % and 96 % for the respective cases (Fig. S11). As expected, the energy consumption of HVAC moves inversely with the set temperature. A 1 °C increase in the

set temperature (25 °C–26 °C) drastically reduces energy consumption. For LD, the 1 °C compromise in thermal comfort leads to only 0.18 % additional energy compared to 11.92 %, relative to the benchmark, while the exposure reduction remains the same. Further increase in set temperature can result in even more energy savings. For example, increasing the set temperature to 27 °C will result in net energy savings of 9.40 % while ensuring the same exposure reduction. A similar reduction in energy consumption from ~96 % (25 °C) to ~68 % (26 °C) is observed for TGD (Fig. S11B). However, even the set temperature of 28 °C does not lead to net energy savings compared to the benchmark owing to high indoor PM concentrations that require the operation of DASS for extended durations. Therefore, a 1 °C change in indoor temperature can yield significant energy savings with comparable exposure reduction. A study on optimizing personal PM exposure and energy consumption via predictive control estimated an average 10.4 % increase in energy consumption to reduce personal exposure by 69 % [45]. However, the study did not account for the average variation of >1 °C in indoor temperatures corresponding to optimization and the benchmark cases. Therefore, it is critical to consider thermal comfort while doing a comparative optimization analysis with benchmarks for an accurate and reliable energy-exposure relationship.

The relationships discussed in Sections 3.1 and 3.2 quantifies the trade-offs among energy, exposure, and thermal comfort. The personal exposure reduction of indoor PM with no compromise in thermal comfort is energy-intensive, while energy savings result in elevated exposure and potentially compromise thermal comfort. In addition to increasing the set temperature, installing air filters in the AHU is another strategy to reduce personal exposure with a lower energy penalty relative to exfiltration [71–74]. The following section presents the results from the simulations performed to investigate the energy-exposure relationship while using filters.

3.3. Impact of AHU filter

As demonstrated in Sections 3.1 and 3.2, exfiltration-dependent strategies for IAP reduction are energy intensive, and previous studies have also reported similar observations [71,72,75–77]. Indoor-outdoor air change might also lead to the infiltration of pollutants of outdoor origin, further worsening IAQ. Therefore, in-duct filters can be an alternative IAP mitigation strategy as explored in previous studies [71, 73,74,78–81]. Filters, especially those with high efficiency, lead to additional energy consumption due to added pressure drop. Depending on the AHU (variable or constant fan speed), the energy consumption may increase or remain constant [82–85].

Simulations are performed assuming a filter is installed in the AHU to

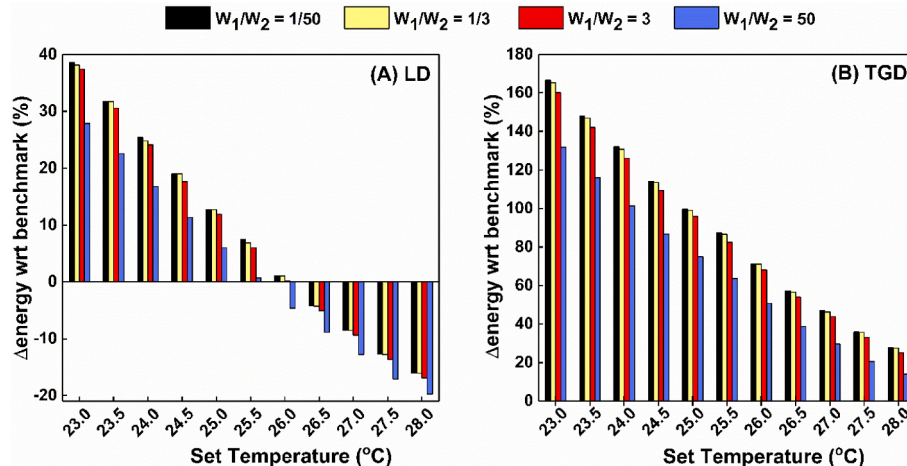


Fig. 3. Change in energy consumption with variations in set temperature for (A) LD and (B) TGD for four W_1/W_2 ratios. (+)ve and (-)ve change means increment and reduction with respect to benchmark, respectively.

clean up recirculating air to assess its efficacy in reducing personal exposure and energy consumption owing to decreased indoor-outdoor air change rate. Based on a survey of commercially available filters, a pressure drop of 87 Pa and particle removal efficiency of 90 % is adopted. A brief discussion on filters is presented in Section S7. The cost of filter installation and replacement is not accounted for here. All simulations are performed for a W_1/W_2 ratio of 3 while keeping all other parameters and constraints similar to previous cases. It is being reiterated that the AHU operated continuously at a constant flow rate equivalent to 8 h^{-1} during benchmark and all simulations. The discussion here includes a comparative analysis of energy and exposure under three scenarios: (1) benchmark (no filter), (2) optimization with an air filter, and (3) optimization without an air filter.

Filters introduce one more PM sink in addition to exfiltration and deposition. Fig. 4 presents the time-resolved bifurcated contribution of exfiltration, deposition, and filtration (if applicable) in the total removal of PM for benchmark and different simulations. The PM removal rate is of the first order for all three mechanisms. Therefore, the removal rate is directly proportional to the indoor-outdoor change rate, surface deposition rate, and recirculation rate for exfiltration, deposition, and filtration, respectively. Therefore, the PM removal by different mechanisms will be governed by DASS and AHU operating conditions. For the cases without filter (benchmark: Fig. 4A and D; and optimization without filter: Fig. 4B and E), exfiltration and deposition are the only active PM sinks. Previous studies have also reported deposition as the major PM sink in case of no or low indoor-outdoor air change rate [9, 86]. For the benchmark cases with a constant indoor-outdoor air change rate of 0.5 h^{-1} , the deposition was the major sink accounting for 78 % (LD) and 72 % (TGD) of the total PM removal. In contrast, deposition accounted for only 44 % (LD) and 16 % (TGD) of total PM removal for the optimization case without an AHU filter. The share of exfiltration increased because the indoor-outdoor air change rate went as high as 10 h^{-1} due to the optimization function governing DASS operation. The results from the simulations performed with an AHU filter (Fig. 4C and F) show that filtration is the major PM sink for both LD (62 %) and TGD (48 %). Adding an AHU filter further diminishes the fraction of PM

removal via deposition to just 15 % (LD) and 9 % (TGD), while the relative share of exfiltration remains comparable (23 % LD and 43 % TGD). The results suggest that filtration enhances the PM removal rate and, therefore, reduces the load on DASS and cooling demand, as discussed subsequently. However, it should be noted that while efficient for indoor PM capture, the internal filtration strategy might not be effective for controlling gaseous indoor pollutants like CO_2 , NO_x , and VOCs. For example, CO_2 concentrations might not be high in residential buildings with low occupancy. However, elevated CO_2 concentrations have been associated with symptoms of sick building syndrome and can indicate insufficient ventilation [32, 87]. Therefore, a high indoor-outdoor air change rate is desirable to reduce indoor CO_2 concentration in high occupancy settings. Moreover, some studies have associated high CO_2 concentrations with cognitive deficiencies [88–91]. However, such associations are inconsistent as other studies [92, 93] reported no significant association between elevated CO_2 concentrations and cognitive deficiencies.

Fig. 5 compares the indoor PM concentration profiles for the optimization (with and without filter) with that of the benchmark. For the benchmark case, the peak PM concentration and cumulative exposure for LD and TGD are $82 \mu\text{g}/\text{m}^3 - 133 \mu\text{g h}/\text{m}^3$ and $297 \mu\text{g}/\text{m}^3 - 844 \mu\text{g h}/\text{m}^3$, respectively. Optimization without any AHU filter leads to a reduction of 53 % and 37 % in the peak concentration and total exposure, respectively, with an energy penalty of 12 % for LD. In contrast, with an air filter, the reductions in the peak concentration and the total exposure are 65 % and 79 %, respectively, with an energy penalty of 21 % (Table 1). The additional energy consumption is associated with the pressure drop across the filter in the AHU that is modeled to be operating continuously, even if indoor concentrations are low. Therefore, there is a scope for further reducing energy consumption without much compromise in exposure reduction. This aspect of AHU operation is discussed next.

Additional PM removal by AHU filter requires less exfiltration for the same degree of exposure reduction and, therefore, lower cooling demand translating to energy savings. Table 1 summarizes the bifurcated energy for the benchmark and optimization (with and without AHU

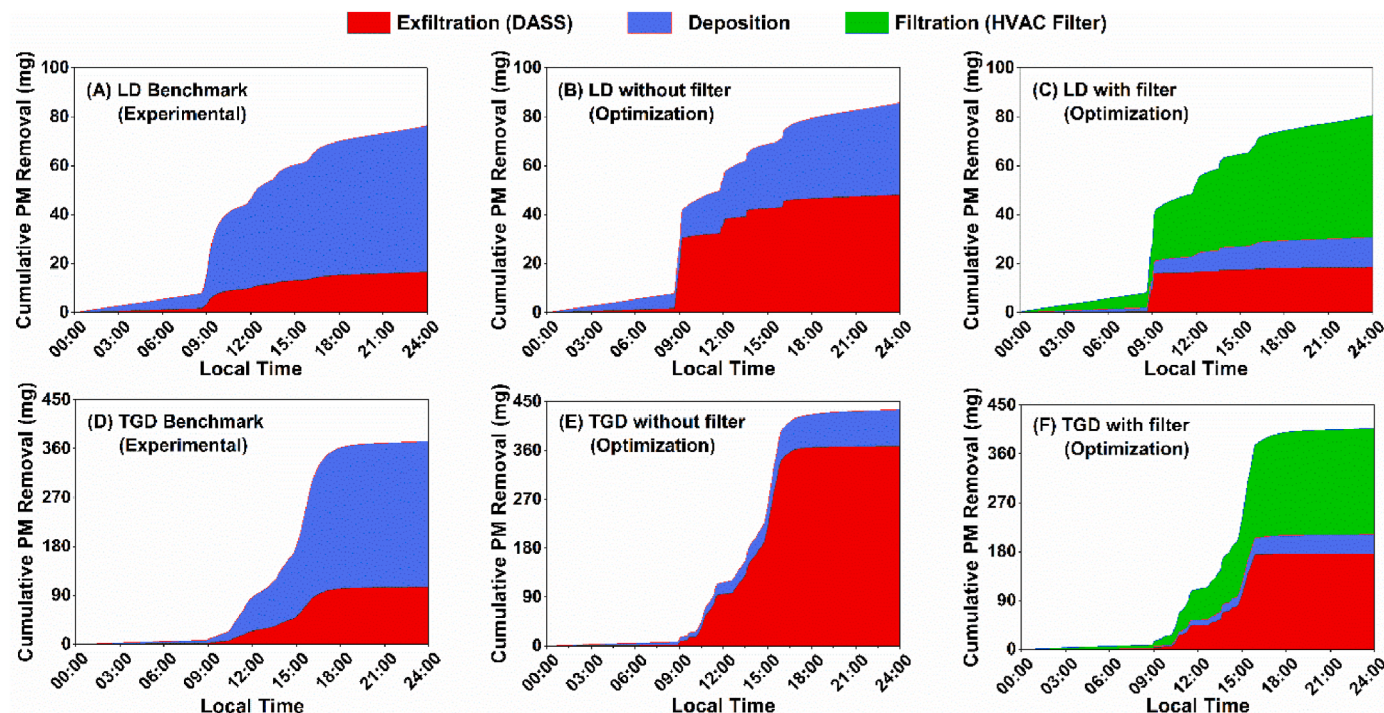


Fig. 4. Bifurcated contribution of three PM removal mechanisms (exfiltration, deposition, and AHU filtration) for the benchmark (A, D) and optimization cases without (B, E) and with AHU filter (C, F). Top and bottom rows correspond to LD and TGD, respectively. All simulations are performed for a W_1/W_2 ratio of 3.

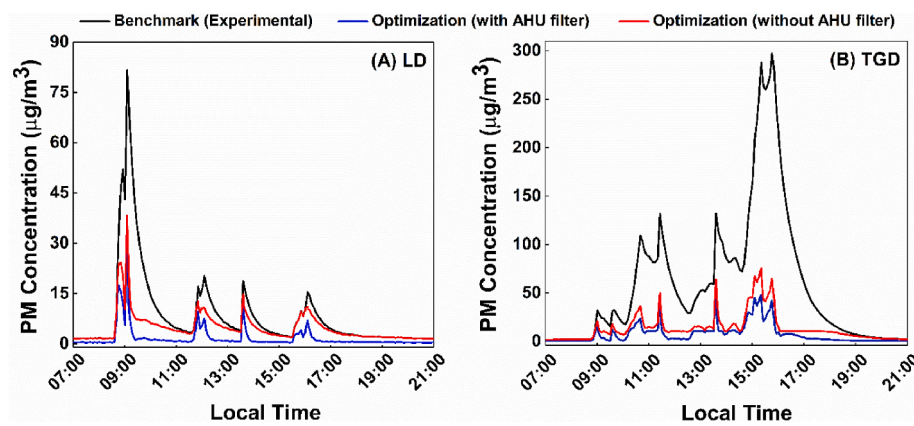


Fig. 5. Temporal indoor PM concentration profiles for the benchmark (experimental; without AHU filter) and the dynamic optimization cases with and without AHU filter for (A) LD and (B) TGD.

Table 1

Bifurcated energy consumption for LD and TGD (benchmark and optimization without and with an air filter) divided into two periods: non-cooking (midnight to 8 a.m. plus 8 p.m. to midnight) and cooking (8 a.m.–8 p.m.). The acronyms used are- AHU (Air Handling Unit), DASS (Dedicated Air Supply System), NER (Normalized Exposure Reduction), and BM (Benchmark).

Activity and Periods	AHU Filter	Energy Consumption (kWh)			Exposure-Energy Nexus	
		DASS	AHU	Cooling Demand	Exposure ($\mu\text{g h m}^{-3}$)	NER
Layered Day (LD)						
Midnight to 8 a.m. + 8 p.m. to midnight (non-cooking)	BM	No	0.13	2.08	1.54	19.52
	Optimization	No	0.13	2.08	1.55	19.52
		Yes	0.13	2.80	1.54	4.88
8 a.m. to 8 p.m. (cooking)	BM	No	0.13	2.09	2.71	113.25
	Optimization	No	0.32	2.09	3.50	64.33
		Yes	0.21	2.82	3.01	22.76
Thanksgiving Day (TGD)						
Midnight to 8 a.m. + 8 p.m. to midnight (non-cooking)	BM	No	0.13	2.08	1.16	25.00
	Optimization	No	0.13	2.08	1.21	24.84
		Yes	0.13	2.80	1.16	4.98
8 a.m. to 8 p.m. (cooking)	BM	No	0.13	2.09	2.66	819.44
	Optimization	No	1.37	2.09	9.29	188.26
		Yes	0.80	2.82	6.24	103.78

filter) cases for two periods: (1) cooking period (8 a.m.–8 p.m.) and (2) non-cooking period (midnight to 8 a.m. + 8 p.m. to midnight). During cooking periods, optimization with the AHU filter leads to higher exposure reduction with comparable or less energy consumption relative to the optimization without the filter. This trend is best reflected by NER (a measure of exposure reduction per unit of additional energy consumed) values for LD (2.18 without filter and 3.55 with filter) and TGD (0.48 without filter and 0.86 with filter). Adding a filter to AHU increased NER for TGD by 79 % compared to just 63 % for LD, indicating that the efficacy of internal filters is more pronounced in high-concentration scenarios. However, the AHU with a filter is modeled to run continuously even though indoor PM concentration is lower than the $10 \mu\text{g}/\text{m}^3$ threshold during non-cooking periods. Therefore, the energy consumption of AHU during cooking and non-cooking periods are the same, but resultant exposure reductions are considerably higher during the cooking period. Therefore, no AHU operation during the non-cooking period of LD can result in an energy savings of 11 % (relative to the benchmark) against the energy penalty of 21 % when AHU is operated continuously, with a filter in both cases (Table 1). Similar trends are observed for TGD too.

Until now, the discussion considers infiltration rates, ambient temperature, and RH corresponding to the location and dates of experiments. In real-world scenarios, the ambient pollutant concentration and weather conditions are dynamic, which will change the dynamics of the optimization problem (Eq. (8)). The next section discusses the impacts of ambient pollution levels and weather conditions on the optimization dynamics.

3.4. Energy-exposure interplay for extreme ambient conditions

The dynamic ambient pollutant concentration governs the infiltration rates at different air change rates, and recent studies demonstrate that indoor exposure to pollutants from outdoor sources constitutes the largest fraction of total exposure. Azimi et al. estimated that 40–60 % of total $\text{PM}_{2.5}$ mortality arises from exposure to $\text{PM}_{2.5}$ of outdoor origin in indoor spaces [36]. Recent studies by Wallace et al. [37] and Lunderberg et al. [38] demonstrated equal contribution of indoor sources in total indoor $\text{PM}_{2.5}$. Other studies have also reported the predominance of pollutants from outdoor origin in indoor environments [3,33–35]. High levels of outdoor pollutant concentrations will translate to high infiltration rates. Hence, the ensuing discussion is on the energy-exposure interplay for scenarios with different infiltration rates than observed during the experiments. For investigating the effect of varying outdoor PM concentrations on the indoor environment, simulations have been performed at seven distinct infiltration rates (IR_{NEW}) compared to the experimental or benchmark (IR_{BM}), i.e., $\text{IR}_{\text{NEW}}/\text{IR}_{\text{BM}} = 0.1, 1, 3, 5, 7, 9$, and 11.

Fig. 6 illustrates the cumulative exposure and energy consumption patterns in two optimization scenarios (with and without an AHU filter) for LD and TGD at different infiltration rates. The total exposure increased linearly ($R^2 > 0.99$) with infiltration rate for LD and TGD in all optimization scenarios (Fig. 6A). For both LD and TGD, exposure without a filter is higher than that with a filter. Without a filter, the PM removal is majorly governed by exfiltration (Fig. 4B and E). However, the outdoor-indoor air change rate also transports outdoor pollutants to

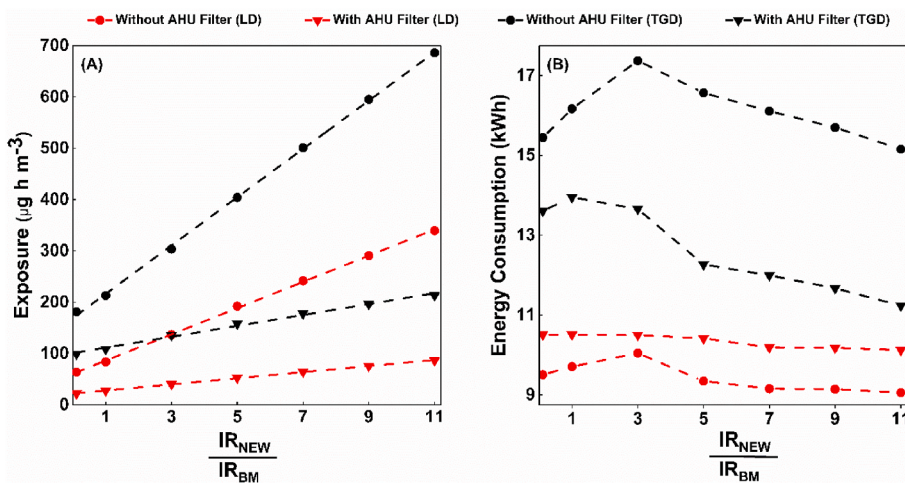


Fig. 6. Variation in (A) exposure and (B) energy consumption with infiltration rates for LD and TGD. All simulations, with and without the AHU filter, are performed for $W_1/W_2 = 3$. IR_{NEW} : assumed infiltration rate for sensitivity analysis and IR_{BM} : infiltration rate derived from experimental data (BM: benchmark).

the indoor space. Therefore, at elevated infiltration rates, the cost function reduces outdoor-indoor air change rate via controlling DASS operation, leading to the accumulation of PM from indoor sources. The exposure increased the fastest with the infiltration rate for TGD without a filter ($5.24 \mu\text{g h m}^{-3}$ per $1 \mu\text{g min}^{-1}$). In contrast, the slowest rate of exposure increase for LD with a filter can be attributed to low indoor PM emissions and the presence of an AHU filter, which dominates the PM removal (Fig. 4C). Even though the PM emissions rates were considerably higher for TGD compared to LD, exposure for TGD with filter are lower than corresponding cases of LD without filter for higher infiltration rates. This observation highlights that AHU filters are critical for not only high IAP but also in areas with high ambient pollution levels.

The energy consumption patterns will also change with varying ambient pollutant levels due to the underlying optimization strategy. As demonstrated in Fig. 6B, the differences in energy consumption with and without a filter at all infiltration rates are lower for LD (mean difference = 0.92 kWh) relative to TGD (mean difference = 3.45 kWh). Further, the energy consumption profiles corresponding to the without filter cases for LD and TGD show a maximum. The observed maxima can be attributed to the changes in optimization dynamics with varying infiltration rates. Up to a specific infiltration rate, PM removal via exfiltration minimizes the cost function even after the associated increase in energy consumption due to increased cooling demand. However, further increases in the infiltration rates favor reduced DASS operation because the higher infiltration rates reduce the efficacy of exfiltration as a removal mechanism. Reduced outdoor-indoor air change rate leads to reduced energy consumption.

For the simulations with a filter, the energy consumption for LD remained in a narrow range (10.1–10.5 kWh) for all infiltration rates owing to the reduced dependency on exfiltration for PM removal (Fig. 4C). With a filter, removal via filtration dominates exposure reduction. Thus, DASS operation is minimized irrespective of infiltration rates reducing cooling demand. Unlike LD, energy consumption for TGD shows sensitivity to infiltration rates even with a filter. Due to much higher emission rates during TGD relative to LD, enhanced operation of DASS is favorable to minimize the cost function even at higher infiltration rates. However, at even higher infiltration rates (not simulated), the energy consumption will become insensitive to infiltration rates like LD.

In summary, this section highlights that in the absence of an AHU filter, (1) exfiltration is the only controllable mechanism for PM removal, though associated with some energy penalty, and (2) the efficacy of exfiltration diminishes for high ambient pollution levels. Internal filtration mechanisms such as an AHU filter provide a more energy-efficient pathway for exposure reduction. An AHU filter

becomes even more critical for high ambient pollution regions.

4. Conclusion

This study demonstrates that optimization-based strategies can effectively mitigate indoor PM exposure while minimizing energy penalty associated with maintaining the thermal comfort of the occupants. The cost function for optimization is governed by the relative importance assigned to the individual objectives (W_1 and W_2), which in turn controls the operation of HVAC and DASS. W_1/W_2 ratio can be modified to achieve desired control over the energy-exposure trade-off. A higher NER (percentage exposure reduction per unit energy penalty), representing a highly energy-efficient system, is desirable. However, high NER values might not always translate to desirable exposure reduction.

For the same cost function, the non-dependence of exposure reduction on the set indoor temperature meant that an increase in the set temperature can significantly reduce the energy penalty while maintaining similar exposure reduction, translating to a higher NER. An increase of just 1 °C in the set temperature reduced the energy penalty (compared to the benchmark) from 11.92 % to 0.18 % for LD and 96 %–68 % for TGD without any considerable compromise with thermal comfort. Therefore, increasing the indoor set temperature can drastically improve NER, but studies focusing on this aspect are limited.

Installation of an AHU filter is another strategy to achieve higher NER while maintaining similar exposure levels. While deposition is the dominant PM removal mechanism for the benchmark case, exfiltration dominated the PM removal for some optimization cases without an AHU filter. With the addition of an AHU filter, filtration became the primary PM removal mechanism. Therefore, similar or even more exposure reduction can be achieved with a lower reliance on exfiltration, translating to air conditioning energy savings. This work assumed constant operation of AHU, but the results suggest that NER can be further improved by implementing a variable operation of AHU. Furthermore, the AHU filters become even more critical for regions with high levels of outdoor air pollution as reliance on exfiltration might also enhance the transport of outdoor pollutants to indoor spaces. Simulations demonstrate that the DASS operation is minimized through the optimization dynamics at high infiltration rates of PM. However, the extent of reduction in DASS operation depends on the relative difference between indoor and outdoor pollution levels. For example, higher emission rates during TGD led to the enhanced operation of DASS even at higher infiltration rates, whereas DASS operation remained closer to the benchmark for LD under the same conditions. Thus, for extreme ambient conditions, filtration via AHU filters is better than exfiltration from the perspective of both energy and personal exposure.

While the size-resolved PM data from expensive research-grade instruments was used, the cumulative mass concentration data calculated using size-resolved data served as the model input for all simulations. With the emergence of low-cost PM sensors that provide cumulative mass concentrations (PM_{1,2,5,10}), this work demonstrates that such sensors, when integrated with the HVAC and DASS, can enable the dynamic operation of these systems to lower personal exposure while minimizing energy penalty.

Unlike this work, which focuses on ambient conditions corresponding to two days during the summer season, future work can consider a range of ambient weather conditions to understand their impacts on the energy-exposure trade-offs, considering extreme temperature events are becoming more frequent. Seasonal variations in the outdoor temperature and RH will affect the optimization dynamics, and heating systems should be included in the model for the winter season. The total energy penalty calculated yearly for varying weather conditions would provide a comprehensive understanding of the energy-exposure trade-off.

Furthermore, the thermal model of the house presented in this work is simplified by assuming no indoor heat sources and a constant value for the thermal permeability of the test house. Future work can include internal heat sources and a more dynamic model for heat transfer between the ambient and the test house. Further studies can also explore the strategy of dynamic indoor set temperatures as an alternative to reduce energy penalty associated with exposure reduction. The current work only considers indoor PM as the governing pollutant, but it can be extended to include other pollutants such as VOCs, NO_x, and CO₂ for a more holistic approach to mitigating IAP.

CRediT authorship contribution statement

Nishchaya Kumar Mishra: Writing – review & editing, Writing – original draft, Visualization, Methodology, Conceptualization. **Marina E. Vance:** Writing – review & editing, Methodology, Funding acquisition, Conceptualization. **Atila Novoselac:** Writing – review & editing, Methodology, Conceptualization. **Sameer Patel:** Writing – review & editing, Writing – original draft, Visualization, Methodology, Funding acquisition, Conceptualization.

Declaration of competing interest

The authors declare that they have no known competing financial interests or personal relationships that could potentially influence the reported work.

Data availability

Data will be made available on request.

Acknowledgments

This work was supported by the Science and Engineering Research Board (SERB), Department of Science and Technology, GoI (Grant# SRG/2021/1001050). The model input data came from the HOMEChem campaign funded by the Alfred P Sloan Foundation (G-2017-9944, G-2016-7050, G-2019-11412, and G-2019-12301). Partial funding from the Indian Institute of Technology Gandhinagar is also acknowledged.

Appendix A. Supplementary data

Supplementary data to this article can be found online at <https://doi.org/10.1016/j.buildenv.2024.111265>.

References

- [1] C. Schweizer, et al., Indoor time-microenvironment-activity patterns in seven regions of Europe, *J. Expo. Sci. Environ. Epidemiol.* 17 (2) (Mar. 2007) 170–181, <https://doi.org/10.1038/SJ.JES.7500490>.
- [2] Indoor Air Quality | US EPA." Accessed: May 11, 2023. [Online]. Available: <https://www.epa.gov/report-environment/indoor-air-quality>.
- [3] A.H. Goldstein, W.W. Nazaroff, C.J. Weschler, J. Williams, How do indoor environments affect air pollution exposure? *Environ. Sci. Technol.* 55 (1) (Jan. 2021) 100–108, https://doi.org/10.1021/ACS.EST.0C05727/ASSET/IMAGES/LARGE/ESOC05727_0001.JPG.
- [4] J.G. Allen, J.D. Macomber, *Healthy Buildings How Indoor Spaces Drive Performance and Productivity*, 2020.
- [5] J.G. Allen, J.D. Macomber, *Healthy Buildings: How Indoor Space Can Make You Sick or Keep You Well*, 2022.
- [6] L. Carmichael, et al., Healthy buildings for a healthy city: is the public health evidence base informing current building policies? *Sci. Total Environ.* 719 (Jun. 2020) 137146 <https://doi.org/10.1016/J.SCITOTENV.2020.137146>.
- [7] J. Saini, M. Dutta, G. Marques, A comprehensive review on indoor air quality monitoring systems for enhanced public health, *Sustainable Environment Research* 30 (1) (Jan. 2020) 1–12, <https://doi.org/10.1186/S42834-020-0047-Y/TABLES/4>.
- [8] K.K. Lee, et al., Adverse health effects associated with household air pollution: a systematic review, meta-analysis, and burden estimation study, *Lancet Glob Health* 8 (11) (Nov. 2020) e1427–e1434, [https://doi.org/10.1016/S2214-109X\(20\)30343-0](https://doi.org/10.1016/S2214-109X(20)30343-0).
- [9] S. Patel, D. Rim, S. Sankhyan, A. Novoselac, M.E. Vance, Aerosol dynamics modeling of sub-500 nm particles during the HOMEChem study, *Environ. Sci. Process Impacts* 23 (11) (Nov. 2021) 1706–1717, <https://doi.org/10.1039/DIELM00259G>.
- [10] S. Patel, et al., Associations between household air pollution and reduced lung function in women and children in rural southern India, *J. Appl. Toxicol.* 38 (11) (Nov. 2018) 1405–1415, <https://doi.org/10.1002/JAT.3659>.
- [11] S. Patel, et al., Indoor particulate matter during HOMEChem: concentrations, size distributions, and exposures, *Environ. Sci. Technol.* 54 (12) (Jun. 2020) 7107–7116, https://doi.org/10.1021/ACS.EST.0C00740/SUPPL_FILE/ESOC00740_LIVESLIDES.MP4.
- [12] L.R. Jia, J. Han, X. Chen, Q.Y. Li, C.C. Lee, Y.H. Fung, Interaction between thermal comfort, indoor air quality and ventilation energy consumption of educational buildings: a comprehensive review, *Buildings* 11 (12) (Nov. 2021) 591, <https://doi.org/10.3390/BUILDINGS11120591>, 2021, Vol. 11, Page 591.
- [13] K. Karyono, B.M. Abdullah, A.J. Cotgrave, A. Bras, The adaptive thermal comfort review from the 1920s, the present, and the future, *Developments in the Built Environment* 4 (Nov. 2020) 100032, <https://doi.org/10.1016/J.DIBE.2020.100032>.
- [14] F. Hou, J. Ma, H.H.L. Kwok, J.C.P. Cheng, Prediction and optimization of thermal comfort, IAQ and energy consumption of typical air-conditioned rooms based on a hybrid prediction model, *Build. Environ.* 225 (Nov. 2022) 109576, <https://doi.org/10.1016/J.BUILDENV.2022.109576>.
- [15] S. Oh, S. Song, Detailed analysis of thermal comfort and indoor air quality using real-time multiple environmental monitoring data for a Childcare center, *Energies* 14 (3) (Jan. 2021) 643, <https://doi.org/10.3390/EN14030643>, 2021, Vol. 14, Page 643.
- [16] J.L. Kephart, et al., Nitrogen dioxide exposures from LPG stoves in a cleaner-cooking intervention trial, *Environ. Int.* 146 (Jan) (2021), <https://doi.org/10.1016/J.ENVINT.2020.106196>.
- [17] J. Usemann, et al., Exposure to moderate air pollution and associations with lung function at school-age: a birth cohort study, *Environ. Int.* 126 (May 2019) 682–689, <https://doi.org/10.1016/J.ENVINT.2018.12.019>.
- [18] K. Yu, et al., Cooking fuels and risk of all-cause and cardiopulmonary mortality in urban China: a prospective cohort study, *Lancet Glob Health* 8 (3) (Mar. 2020) e430–e439, [https://doi.org/10.1016/S2214-109X\(19\)30525-X](https://doi.org/10.1016/S2214-109X(19)30525-X).
- [19] B.S. James, R.S. Shetty, A. Kamath, A. Shetty, Household cooking fuel use and its health effects among rural women in southern India—a cross-sectional study, *PLoS One* 15 (4) (Apr. 2020) e0231757, <https://doi.org/10.1371/JOURNAL.PONE.0231757>.
- [20] WHO, "Household air pollution and health." Accessed: Apr. 20, 2023. [Online]. Available: <https://www.who.int/news-room/fact-sheets/detail/household-air-pollution-and-health>.
- [21] D.E. Schraufnagel, The health effects of ultrafine particles, *Exp. Mol. Med.* 52 (3) (Mar. 2020) 311–317, <https://doi.org/10.1038/s12276-020-0403-3>, 2020 52:3.
- [22] J. Madureira, et al., Assessment of indoor air exposure at residential homes: Inhalation dose and lung deposition of PM10, PM2.5 and ultrafine particles among newborn children and their mothers, *Sci. Total Environ.* 717 (May 2020) 137293, <https://doi.org/10.1016/J.SCITOTENV.2020.137293>.
- [23] B.B. Karakoçak, et al., Biocompatibility of gold nanoparticles in retinal pigment epithelial cell line, *Toxicol. Vitro* 37 (Dec. 2016) 61–69, <https://doi.org/10.1016/J.TIV.2016.08.013>.
- [24] A. Voliotis, C. Samara, Submicron particle number doses in the human respiratory tract: implications for urban traffic and background environments, *Environ. Sci. Pollut. Control Ser.* 25 (33) (Nov. 2018) 33724–33735, <https://doi.org/10.1007/S11356-018-3253-Y/FIGURES/7>.
- [25] H.S. Kwon, M.H. Ryu, C. Carlsten, Ultrafine particles: unique physicochemical properties relevant to health and disease, *Exp. Mol. Med.* 52 (3) (Mar. 2020) 318–328, <https://doi.org/10.1038/s12276-020-0405-1>, 2020 52:3.

- [26] J. Marval, P. Tronville, Ultrafine particles: a review about their health effects, presence, generation, and measurement in indoor environments, *Build. Environ.* 216 (May 2022) 108992, <https://doi.org/10.1016/J.BUILDENV.2022.108992>.
- [27] O. Wayne, W. Lance, Experimental results for fine and ultrafine particles measured in cooking activities, *ISEE Conference Abstracts* 2013 (1) (Sep. 2013), <https://doi.org/10.1289/ISEE.2013.0-4-05-04>.
- [28] R.J. de Dear, G.S. Brager, Thermal comfort in naturally ventilated buildings: revisions to ASHRAE Standard 55, *Energy Build.* 34 (6) (Jul. 2002) 549–561, [https://doi.org/10.1016/S0378-7788\(02\)00005-1](https://doi.org/10.1016/S0378-7788(02)00005-1).
- [29] “Thermal Performance of the Exterior Envelopes of Whole Buildings XII International Conference”.
- [30] P. Northwest National Laboratory, Building America Top Innovations 2014 Profile: ASHRAE Standard 62.2. Ventilation and Acceptable Indoor Air Quality in Low-Rise Residential Buildings, 1995. Accessed: Mar. 07, 2022. [Online]. Available: www.buildingamerica.gov.
- [31] P. Carrer, E. de Oliveira Fernandes, H. Santos, O. Hänninen, S. Kephalaopoulos, P. Wargocki, On the Development of health-based ventilation guidelines: principles and framework, *Int. J. Environ. Res. Publ. Health* 15 (7) (Jun. 2018) 1360, <https://doi.org/10.3390/IJERPH15071360>, 2018, Vol. 15, Page 1360.
- [32] A. Persily, Challenges in developing ventilation and indoor air quality standards: the story of ASHRAE Standard 62, *Build. Environ.* 91 (Sep. 2015) 61–69, <https://doi.org/10.1016/J.BUILDENV.2015.02.026>.
- [33] C.H. Jeong, et al., Indoor measurements of air pollutants in residential houses in urban and suburban areas: indoor versus ambient concentrations, *Sci. Total Environ.* 693 (Nov. 2019) 133446, <https://doi.org/10.1016/J.SCITOTENV.2019.07.252>.
- [34] T.V. Vu, et al., Assessing the contributions of outdoor and indoor sources to air quality in London homes of the SCAMP cohort, *Build. Environ.* 222 (Aug. 2022) 109359, <https://doi.org/10.1016/J.BUILDENV.2022.109359>.
- [35] D.Y.C. Leung, Outdoor-indoor air pollution in urban environment: challenges and opportunity, *Front. Environ. Sci.* 2 (JAN) (Jan. 2015) 119805, <https://doi.org/10.3389/FENVS.2014.00069>/BIBTEX.
- [36] P. Azimi, B. Stephens, A framework for estimating the US mortality burden of fine particulate matter exposure attributable to indoor and outdoor microenvironments, *J. Expo. Sci. Environ. Epidemiol.* 30 (2) (Dec. 2018) 271–284, <https://doi.org/10.1038/s41370-018-0103-4>, 2018 30:2.
- [37] L.A. Wallace, T. Zhao, N.E. Klepeis, Indoor contribution to PM2.5 exposure using all PurpleAir sites in Washington, Oregon, and California, *Indoor Air* 32 (9) (Sep. 2022) e13105, <https://doi.org/10.1111/INA.13105>.
- [38] D.M. Lunderberg, Y. Liang, B.C. Singer, J.S. Apte, W.W. Nazaroff, A.H. Goldstein, Assessing residential PM2.5 concentrations and infiltration factors with high spatiotemporal resolution using crowdsourced sensors, *Proc Natl Acad Sci U S A* 120 (50) (Dec. 2023) e2308832120, <https://doi.org/10.1073/PNAS.2308832120>/SUPPL_FILE/PNAS.2308832120.SAPP.PDF.
- [39] X. Cao, X. Dai, J. Liu, Building energy-consumption status worldwide and the state-of-the-art technologies for zero-energy buildings during the past decade, *Energy Build.* 128 (Sep. 2016) 198–213, <https://doi.org/10.1016/J.ENBUILD.2016.06.089>.
- [40] V. Vakilroaya, B. Samali, A. Fakhar, K. Pishghadam, A review of different strategies for HVAC energy saving, *Energy Convers. Manag.* 77 (Jan. 2014) 738–754, <https://doi.org/10.1016/J.ENCONMAN.2013.10.023>.
- [41] L. Pérez-Lombard, J. Ortiz, C. Pout, A review on buildings energy consumption information, *Energy Build.* 40 (3) (Jan. 2008) 394–398, <https://doi.org/10.1016/J.ENBUILD.2007.03.007>.
- [42] M. Santamouris, K. Vasiliakopoulou, Present and future energy consumption of buildings: challenges and opportunities towards decarbonisation, *e-Prime - Advances in Electrical Engineering, Electronics and Energy* 1 (Jan. 2021) 100002, <https://doi.org/10.1016/J.PRIME.2021.100002>.
- [43] M. González-Torres, L. Pérez-Lombard, J.F. Coronel, I.R. Maestre, D. Yan, A review on buildings energy information: trends, end-uses, fuels and drivers, *Energy Rep.* 8 (Nov. 2022) 626–637, <https://doi.org/10.1016/J.LEGGR.2021.11.280>.
- [44] M. Gholamzadehmir, C. Del Pero, S. Buffa, R. Fedrizzi, N. Aste, Adaptive-predictive control strategy for HVAC systems in smart buildings – a review, *Sustain. Cities Soc.* 63 (Dec. 2020) 102480, <https://doi.org/10.1016/J.SCS.2020.102480>.
- [45] R.S.T. Saini, S.K. Patel, H.S. Ganesh, Energy-focused predictive control for particulate matter concentration and thermal comfort indoors in Delhi, *J. Build. Eng.* 73 (Aug. 2023) 106745, <https://doi.org/10.1016/J.JOBE.2023.106745>.
- [46] H.S. Ganesh, H.E. Fritz, T.F. Edgar, A. Novoselac, M. Baldea, A model-based dynamic optimization strategy for control of indoor air pollutants, *Energy Build.* 195 (Jul. 2019) 168–179, <https://doi.org/10.1016/j.enbuild.2019.04.022>.
- [47] H.S. Ganesh, K. Seo, H.E. Fritz, T.F. Edgar, A. Novoselac, M. Baldea, Indoor air quality and energy management in buildings using combined moving horizon estimation and model predictive control, *J. Build. Eng.* 33 (Jan. 2021), <https://doi.org/10.1016/j.jobe.2020.101552>.
- [48] P.T.M. Tran, M.G. Adam, R. Balasubramanian, Mitigation of indoor human exposure to airborne particles of outdoor origin in an urban environment during haze and non-haze periods, *J. Hazard Mater.* 403 (Feb. 2021) 123555, <https://doi.org/10.1016/J.JHAZMAT.2020.123555>.
- [49] M. Baghoolizadeh, M. Rostamzadeh-Renani, S.A.H.H. Dehkordi, R. Rostamzadeh-Renani, D. Toghraie, A prediction model for CO₂ concentration and multi-objective optimization of CO₂ concentration and annual electricity consumption cost in residential buildings using ANN and GA, *J. Clean. Prod.* 379 (Dec. 2022) 134753, <https://doi.org/10.1016/J.JCLEPRO.2022.134753>.
- [50] H. Liu, et al., Multi-objective optimization of indoor air quality control and energy consumption minimization in a subway ventilation system, *Energy Build.* 66 (Nov. 2013) 553–561, <https://doi.org/10.1016/J.ENBUILD.2013.07.066>.
- [51] X. Xu, B. Fu, Z. Wu, G. Sun, Predictive control for indoor environment based on thermal adaptation, *Sci. Prog.* 104 (2) (Apr. 2021) 1–25, <https://doi.org/10.1177/00368504211006971>.
- [52] D.K. Farmer, et al., Overview of HOMEChem: house observations of microbial and environmental chemistry, *Environ Sci Process Impacts* 21 (8) (Aug. 2019) 1280–1300, <https://doi.org/10.1039/C9EM00228F>.
- [53] C. Arata, et al., Volatile organic compound emissions during HOMEChem, *Indoor Air* 31 (6) (Nov. 2021) 2099–2117, <https://doi.org/10.1111/INA.12906>.
- [54] W.W. Nazaroff, Indoor particle dynamics, *Indoor Air* 14 (SUPPL. 7) (2004) 175–183, <https://doi.org/10.1111/J.1600-0668.2004.00286.X>.
- [55] H. Do, K.S. Cetin, Data-driven evaluation of residential HVAC system efficiency using energy and environmental data, *Energies* 12 (1) (Jan. 2019) 188, <https://doi.org/10.3390/EN12010188>, 2019, Vol. 12, Page 188.
- [56] Engineering Toolbox, “Mixing of Humid Air.” Accessed: May 17, 2023. [Online]. Available: <https://www.engineeringtoolbox.com/mixing-humid-air-d-694.html>.
- [57] A. Afram, P. Janabi-Sharifi, Review of modeling methods for HVAC systems, *Appl. Therm. Eng.* 67 (1–2) (Jun. 2014) 507–519, <https://doi.org/10.1016/J.APPLTHERMALENG.2014.03.055>.
- [58] C. Eley Associates, “Passive Solar Design Strategies: Guidelines for BODLE Building.”
- [59] J. M. P. Sala Lizarraga and A. Picallo-Perez, Exergy Analysis and Thermoeconomics of Buildings : Design and Analysis for Sustainable Energy Systems..
- [60] I. Dinçer and M. (Marc A.) Rosen, Exergy Analysis of Heating, Refrigerating and Air Conditioning : Methods and Applications..
- [61] ASHRAE - iWrapper. Accessed: Dec. 15, 2023. [Online]. Available: https://ashrae.iwrapper.com/ASHRAE_PREVIEW_ONLY_STANDARDS/STD_62.2_2022.
- [62] Weighted Sum Method - an overview | ScienceDirect Topics. Accessed: Jun. 22, 2023. [Online]. Available: <https://www.sciencedirect.com/topics/computer-science/weighted-sum-method>.
- [63] X.-S. Yang, Multi-objective optimization, *Nature-Inspired Optimization Algorithms* (2014) 197–211, <https://doi.org/10.1016/B978-0-12-416743-8.00014-2>.
- [64] G. Serale, M. Fiorentini, A. Capozzoli, D. Bernardini, A. Bemporad, Model predictive control (MPC) for enhancing building and HVAC system energy efficiency: problem formulation, applications and opportunities, *Energies* 11 (3) (Mar. 2018) 631, <https://doi.org/10.3390/EN11030631>, 2018, Vol. 11, Page 631.
- [65] Standard 55 – Thermal Environmental Conditions for Human Occupancy.” Accessed: Jul. 06, 2023. [Online]. Available: <https://www.ashrae.org/technical-resources/bookstore/standard-55-thermal-environmental-conditions-for-human-occupancy>.
- [66] J.A.O. Jose, J.A.O. Jose, A review of general and local thermal comfort models for controlling indoor ambiences, *Air Quality* (Aug. 2010), <https://doi.org/10.5772/9763>.
- [67] S. Jing, B. Li, M. Tan, H. Liu, Impact of Relative Humidity on Thermal Comfort in a Warm Environment 22 (4) (Sep. 2012) 598–607, <https://doi.org/10.1177/1420326X12447614>, 10.1177/1420326X12447614.
- [68] F. Nicol, Adaptive thermal comfort standards in the hot-humid tropics, *Energy Build.* 36 (7) (Jul. 2004) 628–637, <https://doi.org/10.1016/J.ENBUILD.2004.01.016>.
- [69] M. Vellei, M. Herrera, D. Fosas, S. Natarajan, The influence of relative humidity on adaptive thermal comfort, *Build. Environ.* 124 (Nov. 2017) 171–185, <https://doi.org/10.1016/J.BUILDENV.2017.08.005>.
- [70] B. Givoni, Comfort, climate analysis and building design guidelines, *Energy Build.* 18 (1) (Jan. 1992) 11–23, [https://doi.org/10.1016/0378-7788\(92\)90047-K](https://doi.org/10.1016/0378-7788(92)90047-K).
- [71] T. Ben-David, M.S. Waring, Interplay of ventilation and filtration: differential analysis of cost function combining energy use and indoor exposure to PM2.5 and ozone, *Build. Environ.* 128 (Jan. 2018) 320–335, <https://doi.org/10.1016/J.BUILDENV.2017.10.025>.
- [72] T. Ruan, D. Rim, Indoor air pollution in office buildings in mega-cities: effects of filtration efficiency and outdoor air ventilation rates, *Sustain. Cities Soc.* 49 (Aug. 2019) 101609, <https://doi.org/10.1016/J.SCS.2019.101609>.
- [73] T. Li, J.A. Siegel, Assessing the impact of filtration systems in indoor environments with effectiveness, *Build. Environ.* 187 (Jan. 2021) 107389, <https://doi.org/10.1016/J.BUILDENV.2020.107389>.
- [74] T. Ben-David, S. Wang, A. Rackes, M.S. Waring, Measuring the efficacy of HVAC particle filtration over a range of ventilation rates in an office building, *Build. Environ.* 144 (Oct. 2018) 648–656, <https://doi.org/10.1016/J.BUILDENV.2018.08.018>.
- [75] S. Liu, R. Song, T. Tim Zhang, Residential building ventilation in situations with outdoor PM2.5 pollution, *Build. Environ.* 202 (Sep. 2021) 108040, <https://doi.org/10.1016/J.BUILDENV.2021.108040>.
- [76] E.R. Jones, et al., The effects of ventilation and filtration on indoor PM2.5 in office buildings in four countries, *Build. Environ.* 200 (Aug. 2021) 107975, <https://doi.org/10.1016/J.BUILDENV.2021.107975>.
- [77] W.R. Chan, S. Parthasarathy, W.J. Fisk, T.E. McKone, Estimated effect of ventilation and filtration on chronic health risks in U.S. offices, schools, and retail stores, *Indoor Air* 26 (2) (Apr. 2016) 331–343, <https://doi.org/10.1111/INA.12189>.
- [78] B. Stephens, Evaluating the sensitivity of the mass-based particle removal calculations for HVAC filters in ISO 16890 to assumptions for aerosol distributions, *Atmosphere* 9 (3) (Feb. 2018) 85, <https://doi.org/10.3390/ATMOS9030085>, 2018, Vol. 9, Page 85.
- [79] C.A. Faulkner, J.E. Castellini, W. Zuo, D.M. Lorenzetti, M.D. Sohn, Investigation of HVAC operation strategies for office buildings during COVID-19 pandemic, *Build. Environ.* 207 (Jan. 2022) 108519, <https://doi.org/10.1016/J.BUILDENV.2021.108519>.

- [80] M.M. Maestas, et al., Reduction of personal PM2.5 exposure via indoor air filtration systems in Detroit: an intervention study, *J. Expo. Sci. Environ. Epidemiol.* 29 (4) (Nov. 2018) 484–490, <https://doi.org/10.1038/s41370-018-0085-2>, 2018 29:4.
- [81] S. Dubey, H. Rohra, A. Taneja, Assessing effectiveness of air purifiers (HEPA) for controlling indoor particulate pollution, *Heliyon* 7 (9) (Sep. 2021) e07976, <https://doi.org/10.1016/J.HELIYON.2021.E07976>.
- [82] T. Fazli, R.Y. Yeap, B. Stephens, Modeling the energy and cost impacts of excess static pressure in central forced-air heating and air-conditioning systems in single-family residences in the U.S., *Energy Build.* 107 (Nov. 2015) 243–253, <https://doi.org/10.1016/J.ENBUILD.2015.08.026>.
- [83] M. Zaatar, A. Novoselac, J. Siegel, The relationship between filter pressure drop, indoor air quality, and energy consumption in rooftop HVAC units, *Build. Environ.* 73 (Mar. 2014) 151–161, <https://doi.org/10.1016/J.BUILDENV.2013.12.010>.
- [84] B. Stephens, J.A. Siegel, *Energy Implications of Filtration in Residential and Light-Commercial Construction Final Report*, 2010.
- [85] N. Nassif, The impact of air filter pressure drop on the performance of typical air-conditioning systems, *Build. Simul.* 5 (4) (Dec. 2012) 345–350, <https://doi.org/10.1007/S12273-012-0091-6/METRICS>.
- [86] S.G. Jeong, L. Wallace, D. Rim, Contributions of coagulation, deposition, and ventilation to the removal of airborne nanoparticles in indoor environments, *Environ. Sci. Technol.* 55 (14) (Jul. 2021) 9730–9739, <https://doi.org/10.1021/ACS.EST.0C08739>.
- [87] S.D. Lowther, et al., Low level carbon dioxide indoors—a pollution indicator or a pollutant? A health-based perspective, *Environments* 8 (11) (Nov. 2021) 125, <https://doi.org/10.3390/ENVIRONMENTS8110125>, 2021, Vol. 8, Page 125.
- [88] J. González-Martín, N.J.R. Kraakman, C. Pérez, R. Lebrero, R. Muñoz, A state-of-the-art review on indoor air pollution and strategies for indoor air pollution control, *Chemosphere* 262 (Jan. 2021) 128376, <https://doi.org/10.1016/J.CHEMOSPHERE.2020.128376>.
- [89] J. Bartyzel, D. Zieba, J. Necki, M. Zimnoch, Assessment of ventilation efficiency in school classrooms based on indoor-outdoor particulate matter and carbon dioxide measurements, *Sustainability* 12 (14) (Jul. 2020) 5600, <https://doi.org/10.3390/SU12145600>, 2020, Vol. 12, Page 5600.
- [90] B. Du, M.C. Tandoc, M.L. Mack, J.A. Siegel, Indoor CO₂ concentrations and cognitive function: a critical review, *Indoor Air* 30 (6) (Nov. 2020) 1067–1082, <https://doi.org/10.1111/INA.12706>.
- [91] D. Chen, G. Huebner, E. Bagkeris, M. Ucci, D. Mumovic, Effects of exposure to moderate pure carbon dioxide levels on cognitive performance, acute health symptoms and perceived indoor environment quality, *SSRN Electron. J.* (Jun. 2023), <https://doi.org/10.2139/SSRN.4480189>.
- [92] X. Zhang, P. Wargoeki, Z. Lian, C. Thyregod, Effects of exposure to carbon dioxide and bioeffluents on perceived air quality, self-assessed acute health symptoms, and cognitive performance, *Indoor Air* 27 (1) (Jan. 2017) 47–64, <https://doi.org/10.1111/INA.12284>.
- [93] X. Zhang, P. Wargoeki, Z. Lian, Human responses to carbon dioxide, a follow-up study at recommended exposure limits in non-industrial environments, *Build. Environ.* 100 (May 2016) 162–171, <https://doi.org/10.1016/J.BUILDENV.2016.02.014>.